Conversion of laser phase noise to amplitude noise in a resonant atomic vapor: The role of laser linewidth

J. C. Camparo and J. G. Coffer
Mail Stop M2-253, Electronics Technology Center, The Aerospace Corporation, P.O. Box 92957, Los Angeles, California 90009
(Received 16 July 1998)

When laser light propagates through a resonant medium, the transmitted beam can exhibit excess intensity noise [amplitude modulation (AM)]. In a semiclassical description of the phenomenon, laser phase noise (PM) induces fluctuations in the medium's electric susceptibility, which in turn cause fluctuations in the transmitted intensity. The process provides an efficient means for PM-to-AM conversion, and intuition suggests that large linewidth lasers should exhibit much greater PM-to-AM conversion than narrow linewidth lasers. Here we measure the relative intensity noise (RIN) for two diode lasers whose linewidths $\Delta\nu_L$ differ by more than 10^2, after the lasers have propagated through a resonant rubidium vapor. Though the RIN of the narrow linewidth laser is only reduced by a factor of about 6 compared to the broad linewidth laser, our results are nonetheless consistent with numerical simulations of the PM-to-AM conversion process. In particular, both computation and analytical theory indicate that RIN is a nonlinear function of $\Delta\nu_L$. For single-mode laser linewidths less than the atomic dephasing rate, RIN increases like $\sqrt{\Delta\nu_L}$, while for linewidths greater than the atomic dephasing rate RIN is a *decreasing* function of $\Delta\nu_L$. [S1050-2947(99)00901-4]

PACS number(s): 42.50.Gy, 42.62.Fi, 42.25.Bs

I. INTRODUCTION

It is now fairly well established that when laser light propagates through a resonant medium, the transmitted beam will exhibit some level of excess intensity noise. Though the phenomenon may be modeled in different ways, depending on the specifics of the experimental situation, in all cases the excess intensity noise results from a mapping of atomic fluctuations onto the resonant optical field. In strong fields, where the transition may be saturated, this phenomenon is described using a quantum electrodynamics formalism, and is explained as ''vacuum side-mode amplification due to forward four-wave mixing'' [1]. In this regime, the phenomenon can be quite significant even for perfectly monochromatic fields, as a consequence of the medium's natural relaxation processes, and it plays a role in certain amplitude-squeezing experiments [2]. In weak fields the phenomenon is no less important, though it is primarily associated with the laser's intrinsic phase fluctuations, and can be explained semiclassically: laser phase noise (PM) induces fluctuations in the medium's electric susceptibility, which in turn cause fluctuations in the laser's transmitted intensity [amplitude modulation (AM)] [3]. At high Fourier frequencies, the weak-field manifestation of the phenomenon provides spectroscopic information on the resonant medium's energy level structure, as first reported by Yabuzaki *et al.* [4]. In optically thick media, the low Fourier frequency components of the excess intensity noise can be orders of magnitude larger than the laser's intrinsic relative intensity noise, and the PM-to-AM conversion phenomenon becomes an important physical process limiting the performance of gas-cell atomic clocks [5,6].

The present studies consider the role of single-mode laser linewidth in the PM-to-AM conversion process for weak fields. Intuitively, one expects the magnitude of PM-to-AM conversion to scale with linewidth, since a single-mode laser's linewidth is principally related to the laser's phase noise. In particular, as suggested by the high Fourier frequency experiments of McLean *et al.* [7] and McIntyre *et al.* [8], if the linewidth of a diode laser is narrowed by several orders of magnitude, one anticipates orders of magnitude reduction in processes associated with PM-to-AM conversion. The experimental and theoretical results described below, however, do not completely bear out this expectation. In Sec. II we describe an experiment that compares the relative intensity noise (RIN) of two diode lasers whose linewidths differ by two orders of magnitude. The measurements were performed for several different values of the vapor's optical depth. On average, the RIN of the narrowed diode laser was at best only a factor $\sim$6 smaller than the RIN of the much broader diode laser. As discussed in Sec. IV, these observations are consistent with numerical simulations of the PM-to-AM conversion process, which additionally show that for large linewidth fields RIN is a *decreasing* function of laser linewidth. The computational results are elucidated in Sec. V, where it is shown that the variance of atomic coherence fluctuations, which drive the PM-to-AM conversion process, has a maximum when the laser linewidth equals the optical transition's homogeneous linewidth.

II. EXPERIMENT

Figure 1 shows a block diagram of the experimental arrangement. The beams from a Mitsubishi TJS [9] AlGaAs diode laser (ML4102) and an EOSI [10] external cavity (EC) AlGaAs diode laser were superimposed, expanded, and allowed to pass through a natural Rb vapor contained within a Pyrex resonance cell (72% Rb^{85} and 28% Rb^{87}) [11]. Only one beam was allowed to pass through the vapor at a time, and both lasers were tuned to the Rb^{85} D_1 transition at 794.7 nm [i.e., $5\ ^2S_{1/2}(F=2)\rightarrow 5\ ^2P_{1/2}(F=2,3)$]. As a result of Doppler broadening, the excited-state hyperfine structure of Rb^{85} was not resolved. The absorption spectrum of the natural vapor, as measured by the TJS diode laser, is shown in Fig. 2(a). The absorption feature of interest for the present work is labeled as *D* in the figure, and is well resolved from

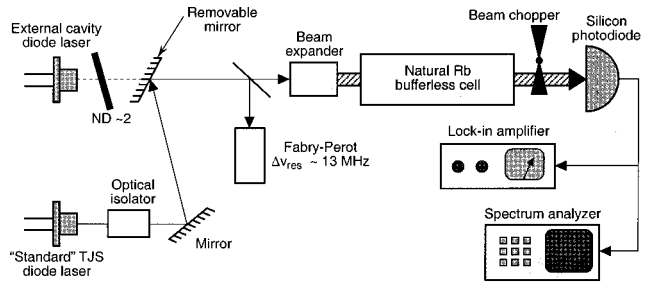

FIG. 1. Experimental arrangement as described in the text.

the other absorption features. An optical isolator, providing at least 36-dB isolation, prevented optical feedback from perturbing the TJS laser's characteristics, while this function was essentially performed by a 2.0 neutral density filter that was tilted and placed in front of the external cavity diode laser. Prior to entering the resonance cell, a portion of laser light was detected with a moderately high finesse confocal Fabry-Perot interferometer (frequency resolution, $\Delta\nu_{\rm res}$, $\sim$13 MHz). The interferometer allowed us to measure the laser detuning from resonance, and also ensured that optical feedback was not artificially broadening either laser's spectrum during the course of the measurements.

The TJS laser had a measured linewidth [full width at half maximum (FWHM)], $\Delta\nu_L$, of 56 MHz. Using a very high finesse confocal interferometer ($\Delta\nu_{\rm res}$, $\sim$0.8 MHz) we measured the external cavity laser linewidth, and found it to be limited by the interferometer resolution. According to the external cavity laser's specifications, the linewidth should be 100 kHz or less. Thus the two lasers had linewidths that differed by at least of factor of 70, and quite likely by nearly three orders of magnitude.

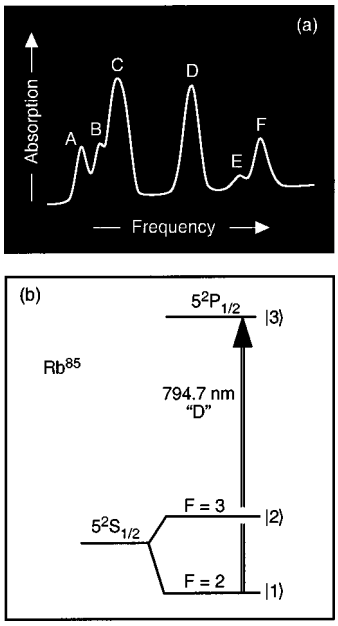

FIG. 2. (a) Absorption spectrum of the natural Rb vapor (i.e., 72% Rb^{85} and 28% Rb^{87}) as measured with the 56-MHz linewidth diode laser at 794.7 nm and at a temperature of 32 °C: (*A*) $5\ ^2P_{1/2}(F=1)\rightarrow 5\ ^2S_{1/2}(F=2)$ transition for Rb^{87}; (*B*) $5\ ^2P_{1/2}(F=2)\rightarrow 5\ ^2S_{1/2}(F=2)$ transition for Rb^{87}; (*C*) $5\ ^2P_{1/2}(F=2,3)\rightarrow 5\ ^2S_{1/2}(F=3)$ transition for Rb^{85}; (*D*) $5\ ^2P_{1/2}(F=2,3)\rightarrow 5\ ^2S_{1/2}(F=2)$ transition for Rb^{85}; (*E*) $5\ ^2P_{1/2}(F=1)\rightarrow 5\ ^2S_{1/2}(F=1)$ transition for Rb^{87}; (*F*) $5\ ^2P_{1/2}(F=2)\rightarrow 5\ ^2S_{1/2}(F=1)$ transition for Rb^{87}. The ground-state hyperfine splitting of Rb^{85} is 3036 MHz, while that of Rb^{87} is 6835 MHz. The $5\ ^2P_{1/2}$ excited-state hyperfine splitting of Rb^{85} is 362 MHz, and unresolved within the Doppler-broadened absorption line, while that of Rb^{87} is 812 MHz. (b) Relevant energy-level diagram for the *D* transition of (a).

The laser power for both beams was 15 μW, measured prior to the resonance cell, and both beams were expanded and then apertured to a diameter of 0.4 cm. The low light intensity in the resonance cell ensured that neither laser could cause any saturation of the optical transition. Additionally, since there was no buffer gas in the resonance cell, there were no confounding effects of optical pumping on PM-to-AM conversion [12,13]. The resonance cell had a length L of 15 cm and a diameter of 2 cm, and was heated by braided wire. For our experiments, the Doppler-broadened linewidth was $\sim$510 MHz, and the natural linewidth of the D_1 transition is 5.67 MHz [14].

In order to be sure that the laser beam's passage through the resonance cell had no appreciable effect on the laser spectrum, we replaced the beam chopper and photodiode shown in Fig. 1 with one of our two interferometers. We then measured the linewidth of the TJS laser (using the interferometer with $\Delta\nu_{\rm res}=13$ MHz) and the EC laser (using the interferometer with $\Delta\nu_{\rm res}\sim 0.8$ MHz) after passage through the vapor. For a vapor temperature of 38 °C, and for the lasers tuned both off resonance and on resonance, the laser linewidths after passage were indistinguishable from the linewidths measured prior to passage through the resonance cell.

The vapor cell temperature was varied from 22 to 46 °C, and for these temperatures the transmission of the external cavity laser was used to estimate the vapor's optical depth τ_d: $\tau_d^{-1}=L^{-1}\ln[I_{\rm off}/I_{\rm on}]$, where subscripts refer to the laser tuned either off or on resonance. For this temperature range, τ_d/L varied from about 3 to 0.3, indicating a transition from an optically thin vapor to an optically thick vapor.

The average laser intensity $\langle I\rangle_{\rm meas}$ was obtained by chopping the light beam and measuring the photodiode signal with a lock-in amplifier. Then the chopper was stopped, and the intensity noise δI in a 1-Hz bandwidth at 1 kHz was measured with a spectrum analyzer that had a 25-kHz bandwidth. The laser RIN was defined as the ratio of δI to $\langle I\rangle$ (where $\langle I\rangle$ corresponds to the measured average laser intensity corrected for amplified spontaneous emission as discussed subsequently), and in all measurements δI was measurably larger than the photodetector's dark noise. (Though this definition of the RIN is essentially the square root of that typically found in the diode laser literature, in our opinion it is more amenable to spectroscopic applications.)

In order to obtain an appropriate value of the RIN for each of the lasers, it was necessary to correct the TJS laser's transmitted intensity for amplified spontaneous emission (ASE). (This correction was also performed for the EC laser, but it was of less significance.) As the gain curve of a diode laser is fairly broad, diode laser Fabry-Perot modes near the main lasing mode will be amplified when the laser is operating above threshold [15]. For the TJS laser, these modes are spaced by about 0.3 nm, and so will not be absorbed by

TABLE I. Ratio of ASE to the transmitted intensity for the lasers tuned on resonance. [This relatively large value is simply due to strong absorption of the EC laser at 46 °C (i.e., $L/t\tau_d = 3.8$).]

	TJS Laser	EC Laser
$\langle I\rangle_{\mathrm{ASE}}/\langle I\rangle_{\mathrm{meas}}$ at 22 °C	0.17	0.01
$\langle I\rangle_{\mathrm{ASE}}/\langle I\rangle_{\mathrm{meas}}$ at 32 °C	0.31	0.02
$\langle I\rangle_{\mathrm{ASE}}/\langle I\rangle_{\mathrm{meas}}$ at 38 °C	0.49	0.05
$\langle I\rangle_{\mathrm{ASE}}/\langle I\rangle_{\mathrm{meas}}$ at 46 °C	0.79	0.38[a]

the vapor when the main lasing mode is tuned on resonance. In our measurements of the RIN, we were interested in the ratio of the intensity fluctuations to the intensity of the main laser mode, which was the mode interacting with the atoms in the vapor. Thus defining $\langle I\rangle_{\mathrm{ASE}}$ as an estimate of the laser's amplified spontaneous emission, we employed $\langle I\rangle = \langle I\rangle_{\mathrm{meas}} - \langle I\rangle_{\mathrm{ASE}}$ in the definition of the RIN noted above. We estimated the magnitude of the ASE by increasing the vapor cell temperature to 56 °C, and then measuring the transmitted intensity of each laser. Using the optical depth measurements from the lower temperatures, we were able to infer that the optical depth at 56 °C was approximately 1 cm, short enough so that no intensity from either laser's main mode should have passed through the vapor. We found that the TJS laser's amplified spontaneous emission was about 11% of the total laser's output [16], while the EC laser's ASE was only about 1% of the total output intensity. Table I shows the *on-resonance* values of $\langle I\rangle_{\mathrm{ASE}}/\langle I\rangle_{\mathrm{meas}}$ for each of the lasers at the four temperatures studied.

III. RESULTS

Figure 3 shows the measured RIN of the two lasers as a function of laser detuning for four different temperatures. At low temperatures, where the vapor is optically thin, the RIN displays a double-peaked dependence on laser detuning. Heuristically, if $L(\nu\text{-}\nu_0)$ is defined as the absorption line shape centered at ν_0, then for PM-to-AM conversion we expect

$$(\delta I/\langle I\rangle) \approx \langle \delta\nu_L\rangle_{\mathrm{rms}} \left|\frac{dL}{d\nu}\right|, \tag{1}$$

where $\langle \delta\nu_L\rangle_{\mathrm{rms}}$ corresponds to the laser's root-mean-square frequency fluctuations. In words, the laser's phase fluctuations cause the laser frequency to vary stochastically across the atom's absorption profile, and as a consequence the amount of light transmitted by the vapor becomes a stochastic quantity. The absolute value of the absorption line shape's derivative implies a double-peaked curve for PM-to-AM conversion RIN as a function of laser detuning, and given the excited-state hyperfine structure associated with this transition, the double-peaked structure could be expected to exhibit some asymmetry. The important point of this observation is that neither shot noise nor the laser's intrinsic RIN would be expected to exhibit such a double-peaked structure [17]. Consequently, the double-peaked appearance of the RIN data shown in Fig. 3, along with the inverse relationship between the magnitude of the RIN and the vapor's optical depth, provide strong evidence that our measurements of the RIN are indeed probing the PM-to-AM conversion process.

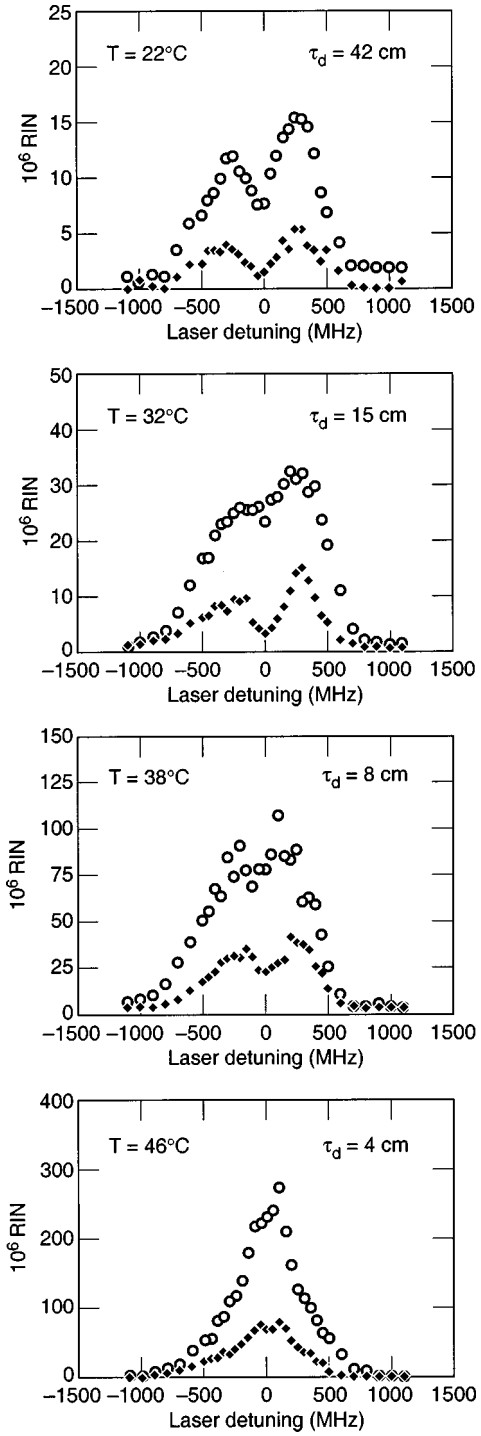

FIG. 3. RIN (multiplied by 10^6) vs laser detuning. Black diamonds correspond to the results obtained with the EC laser, while circles correspond to the results obtained with the TJS diode laser.

One of the more intriguing aspects of Fig. 3 concerns the relative magnitude of the RIN for the two lasers. Given that the linewidths of the two lasers differed by about 10^2 to 10^3, we had originally anticipated that the RIN of the EC laser would be insignificant on the scale of the RIN for the TJS laser. Specifically, since $\langle \delta\nu_L\rangle_{\mathrm{rms}}$ for a singlemode laser with a nearly Lorentzian line shape scales like $\sqrt{\Delta\nu_L}$ [18], all

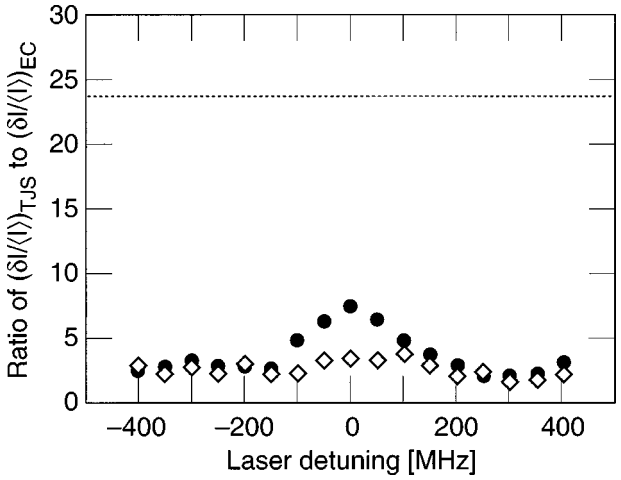

FIG. 4. Ratio of the TJS laser's RIN to that of the EC laser: open triangles correspond to $T=38\,^{\circ}\mathrm{C}$, while filled circles correspond to $T=32\,^{\circ}\mathrm{C}$. The dashed line corresponds to the anticipated value for this ratio based on an EC laser linewidth of 100 kHz.

other things being equal, Eq. (1) implies

$$\frac{(\delta I/\langle I\rangle)_{\mathrm{TJS}}}{(\delta I/\langle I\rangle)_{\mathrm{EC}}}=\left(\frac{\Delta\nu_L^{\mathrm{TJS}}}{\Delta\nu_L^{\mathrm{EC}}}\right)^{1/2}. \tag{2}$$

At a minimum, we therefore expected this ratio to be ~ 10, and quite likely to be nearer to 25 given the EC laser's specified 100-kHz linewidth. Moreover, this ratio was expected to be independent of laser detuning from resonance. As illustrated in Fig. 4, however, when we examined the experimental ratio of the $\mathrm{RIN}_{\mathrm{TJS}}$ to $\mathrm{RIN}_{\mathrm{EC}}$, we found that on average this ratio was ~ 6 for the lasers tuned on resonance, while off resonance this ratio dropped to ~ 3. Thus, while the efficiency of PM-to-AM conversion is certainly a function of laser linewidth, the experimental data indicates that the heuristic description of PM-to-AM conversion embodied by Eq. (1) overly simplifies the fundamental physical process.

IV. COMPUTATION

In the regime of weak fields, such that the optical transition is not saturated, PM-to-AM conversion in optically thick vapors can be described semiclassically [13]. Basically, for a three-level atom like that shown in Fig. 2(b), where optical pumping may be operative, laser phase fluctuations cause fluctuations in the real and imaginary components of the density-matrix coherence σ_{31}. Since the coherence is related to the vapor's electric susceptibility χ, these laser-induced atomic coherence fluctuations essentially result in fluctuations of the vapor's absorption cross section.

Defining u and v as the real and imaginary components of σ_{31}, respectively, and σ_{ii} as the population in $|i\rangle$, it is possible to write the density-matrix components in terms of their average values, and laser-induced fluctuations, $\delta_x(t)$:

$$\sigma_{11}=\Sigma+\delta_\sigma(t), \tag{3a}$$

$$u=u_0+\delta_u(t), \tag{3b}$$

$$v=v_0+\delta_v(t). \tag{3c}$$

As discussed in Ref. [13], the average values are given by

$$\Sigma=\frac{4\gamma_{\mathrm{hfs}}(\Gamma_a\Gamma_b+\Delta^2)}{[8\gamma_{\mathrm{hfs}}(\Gamma_a\Gamma_b+\Delta^2)+\Gamma_a\bar{\Omega}^2]}, \tag{4a}$$

$$u_0=\frac{2\bar{\Omega}\Delta\gamma_{\mathrm{hfs}}}{[8\gamma_{\mathrm{hfs}}(\Gamma_a\Gamma_b+\Delta^2)+\Gamma_a\bar{\Omega}^2]}, \tag{4b}$$

$$v_0=\frac{-2\bar{\Omega}\Gamma_a\gamma_{\mathrm{hfs}}}{[8\gamma_{\mathrm{hfs}}(\Gamma_a\Gamma_b+\Delta^2)+\Gamma_a\bar{\Omega}^2]}, \tag{4c}$$

where

$$\Gamma_a=\Gamma_{\mathrm{col}}+\frac{A}{2}+\gamma, \tag{4d}$$

$$\Gamma_b=\Gamma_{\mathrm{col}}+\frac{A}{2}+\frac{\bar{\Omega}^2}{2A}+\gamma; \tag{4e}$$

while the laser induced fluctuations are described by the following set of stochastic differential equations:

$$\dot{\delta}_\sigma=\frac{\Omega(t)}{2}\,\delta_v-2\gamma_{\mathrm{hfs}}\delta_\sigma, \tag{5a}$$

$$\dot{\delta}_u=-\left(\Gamma_{\mathrm{col}}+\frac{A}{2}\right)\delta_u+\gamma u_0-(\Delta+\delta\omega)\,\delta_v-\delta\omega v_0, \tag{5b}$$

$$\dot{\delta}_v=-\left(\Gamma_{\mathrm{col}}+\frac{A}{2}+\frac{\Omega(t)^2}{2A}\right)\delta_v+\gamma v_0+(\Delta+\delta\omega)\,\delta_u+\delta\omega u_0-\frac{\Omega(t)}{2}\,\delta_\sigma. \tag{5c}$$

In these expressions, Γ_{col} is the collisional dephasing rate of the optical transitions; A is the Einstein A coefficient for the excited state; ω_0 is the average laser frequency, while $\delta\omega$ represents the laser's stochastic frequency fluctuation; 2γ represents the linewidth of the laser (as will be discussed subsequently); $\Delta\equiv(\omega_0-\omega_{31})$; γ_{hfs} is the hyperfine relaxation rate between $|2\rangle$ and $|1\rangle$; and Ω is the optical Rabi frequency. Note that in Eqs. (4) the average value of the Rabi frequency, $\bar{\Omega}$, is employed, while in Eqs. (5) the Rabi frequency is allowed to take on the characteristics of a stochastically varying parameter.

The frequency and *intrinsic* amplitude fluctuations of the laser are modeled as Ornstein-Uhlenbeck processes [19]. Specifically, if $\Omega(z=0,t)$ is defined as the Rabi frequency at the entrance to the resonance cell at time t, then

$$\Omega(0,t)=\bar{\Omega}(0)[1+x(t)], \tag{6a}$$

$$\langle x(t)x(t+\tau)\rangle=\frac{\gamma}{\omega_1}\exp(-\omega_1|\tau|), \tag{6b}$$

$$\langle\delta\omega(t)\,\delta\omega(t+\tau)\rangle=\gamma\beta\,\exp(-\beta|\tau|), \tag{6c}$$

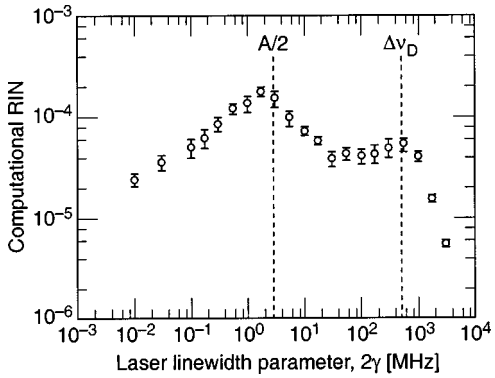

FIG. 5. Computational results of the RIN vs the laser linewidth parameter 2γ. $A/2$ is the optical dephasing rate due to spontaneous emission, while $\Delta\nu_D$ is the Doppler linewidth (FWHM).

TABLE II. Parameters employed in the numerical simulation.

Parameter	Value
Laser input intensity	1 μW/cm^2
Resonance cell temperature	40 °C
Resonance cell length	3 cm
Rubidium vapor pressure	2.9×10^{-6} torr
Estimated τ_d for $2\gamma=0.1$ MHz	1.35 cm
Residual N_2 buffer gas pressure	10^{-6} torr
$\Delta\nu_{\text{Doppler}}$	512 MHz
$\Delta\nu_{\text{Natural}}$	5.67 MHz
Laser intrinsic RIN	10^{-10}
Laser β parameter	3 GHz
δz for computation	0.03 cm

where $\bar{\Omega}(0)$ is the average Rabi frequency at the resonance cell entrance; β^{-1} is the correlation time of laser frequency fluctuations; 2γ is essentially the linewidth of the laser for our nearly Lorentzian line shapes (i.e., $\gamma<\beta$), and $1/\omega_1$ is the correlation time of the laser's intrinsic amplitude fluctuations. Note that in this model, the laser's intrinsic RIN in a 1-Hz bandwidth is $4\sqrt{\gamma}/\omega_1$.

The above density-matrix equations are a function of propagation distance into the vapor cell, z, and, as discussed more fully in Ref. [13], they are solved iteratively to propagate the electric field amplitude through the vapor. Briefly, for a small increment in propagation distance, δz, the laser electric field E can be expanded in a Taylor series:

$$E(z+\delta z)=E(z)-4kN\mu_{13}\langle(v_0+\delta_v)\rangle_v\delta z, \qquad (7)$$

where N is the number density of atoms in the vapor, μ_{13} is the $|1\rangle-|3\rangle$ electric dipole moment, k is the wave vector of the laser light, and $\langle\cdots\rangle_v$ implies a velocity average over the Maxwell-Boltzmann distribution. At various computational time steps, values for the stochastic laser electric-field amplitude and frequency at $z=0$ are determined by the methodology of Camparo and Lambropoulos [20]. The propagation of this wave front through the medium is then determined with the aid of Eqs. (4), (5), and (7). Equations (5) are solved at each position z by a fifth-order Runge-Kutta-Fehlberg method with adaptive (temporal) step size [21], and the step size is restricted so that it is always smaller than $0.1A^{-1}$ and $0.1\Gamma_{\text{col}}^{-1}$. Ten sets of density matrix equations are solved at each position z, corresponding to specific velocity subgroups. The attenuation coefficient (i.e., $\delta E/\delta z$) is averaged over the Doppler distribution by use of Gaussian quadrature [22], and the field is then propagated through the atomic vapor. The intensity of the laser at the exit of the medium is averaged over a time interval equal to the smaller of either A^{-1} or Γ_{col}^{-1}, and is then subjected to statistical analysis to determine δI in a 1-Hz bandwidth at low Fourier frequency.

The results from this one dimensional model are shown in Fig. 5, where the computed RIN is shown as a function of the laser linewidth parameter 2γ. Other parameters used in these calculations are collected in Table II, where it is to be noted that τ_d/L for a 100-kHz linewidth laser is 0.45. The error bars shown in Fig. 5 correspond to our uncertainty in estimating the spectral density of amplitude fluctuations for the transmitted beam, as discussed in Ref. [13].

Perhaps the most striking feature of Fig. 5 is that it predicts that the RIN is a nonmonotonic function of laser linewidth. Though the RIN increases like $\sqrt{\gamma}$ for linewidths less than the atoms' intrinsic dephasing rate, in this case $A/2$, for larger linewidth lasers the RIN is actually a decreasing function of γ. In particular, comparing a 100-kHz linewidth laser with a 60-MHz linewidth laser, a $\sqrt{\gamma}$ dependence would predict that the narrow linewidth laser should have a RIN approximately 25 times smaller than that of the broad linewidth laser. However, the data of Fig. 5 actually indicate that a 100-kHz laser may exhibit nearly the same RIN as a 60-MHz laser, in reasonable agreement with the experimental data of Fig. 4, where the ratio of the RIN values on resonance is about 3 for $T=38$ °C (i.e., $\tau_d/L=0.53$).

In order to pursue the origin of this nonmonotonic dependence, it is necessary to recognize that the RIN depends on a ratio of noise to transmitted light intensity. For the data of Fig. 5, these are displayed separately in Fig. 6. Figure 6(a) shows the average transmitted light intensity as a function of laser linewidth. As might be expected, for laser linewidths less than the homogeneous linewidth, optical transmission increases with γ (i.e., the peak absorption cross section decreases as the laser phase noise adds to the atom's total dephasing rate). However, once the laser linewidth increases beyond the homogeneous width, it interacts with a greater number of velocity subgroups, leading to increased absorption by the vapor. Eventually, when the laser linewidth becomes greater than the Doppler width, the transmitted intensity again increases. Note, however, that the RIN is inversely proportional to the transmitted light intensity, so that taken by itself Fig. 6(a) would predict that the RIN is a *minimum* for linewidths near $A/2$. Figure 6(b) shows the noise level of the transmitted light intensity as a function of laser linewidth. The data points correspond to the noise values used in the computation of the RIN for Fig. 5; the solid line will be discussed subsequently. Clearly, the striking feature of Fig. 6(b) is the ''fall-off'' of PM-to-AM conversion noise for laser linewidths greater than the optical dephasing rate, $A/2$. Together, Figs. 6(a) and 6(b) indicate that the nonmonotonic nature of the RIN for linewidths near $A/2$ results primarily from a nonmonotonic relationship between the efficiency of PM-to-AM conversion noise and laser linewidth. Addition-

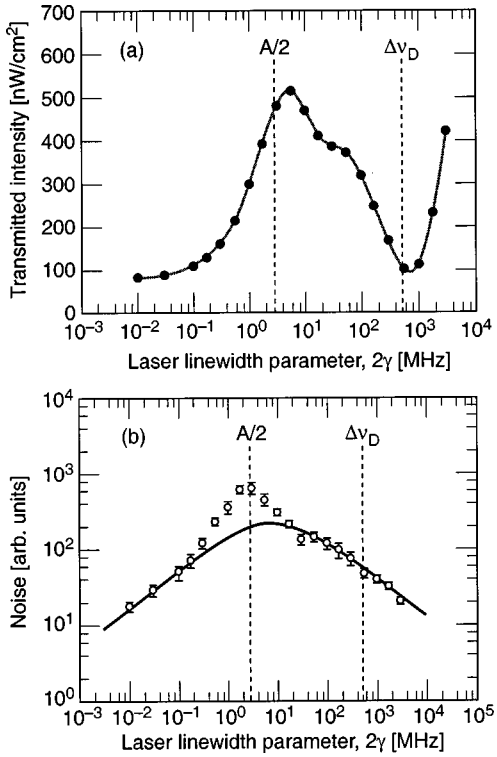

FIG. 6. (a) Filled circles correspond to the computed average transmitted intensity as a function of the laser linewidth parameter. (b) Circles correspond to the computed transmitted intensity noise as a function of the laser linewidth parameter, while the solid line corresponds to the analytical result as discussed in the text.

ally, the drastic reduction of the RIN for linewidths greater than the Doppler width results primarily from the increased optical transmission by the vapor.

V. ANALYSIS

In this section we consider the origin of the nonmonotonic relationship between the efficiency of PM-to-AM conversion noise and laser linewidth. To this end, we note that PM-to-AM conversion derives principally from fluctuations in the atomic coherence [13], and we anticipate from Eq. (7) that the stochastic variations of transmitted intensity will be proportional to the stochastic variations in the coherence. Specifically, assuming that the coherence is approximately constant along the propagation path at any instant, Eq. (7) yields

$$I(L,t)=\langle I(L)\rangle \exp[-8kN\mu_{13}\langle \delta_v(t)\rangle_v L], \tag{8a}$$

where

$$\langle I(L)\rangle \equiv I_0 \exp[-8kN\mu_{13}\langle v_0\rangle_v L]. \tag{8b}$$

For the situations of practical interest (i.e., spectroscopy and atomic clocks), we can further assume that the coherence fluctuations are relatively small, so that the exponential of Eq. (8a) may be expanded. It is then clear that $\delta I(L,t) \sim \langle \delta_v(t)\rangle_v$.

To proceed, we restrict our consideration to fairly weak fields such that $\Omega \ll \gamma_{\rm hfs}$ implying that $\Sigma=\frac{1}{2}$, $\delta_\sigma=0$, and $\Gamma_a \cong \Gamma_b \equiv \Gamma$. Thus defining $\zeta(t)$ as $(\delta_u + i\delta_v)$ and ζ_0 as $\langle \sigma_{13}\rangle$, Eqs. (5) result in

$$\dot{\zeta}=-[\Gamma - i(\Delta+\delta\omega)]\zeta + (\gamma + i\delta\omega)\zeta_0. \tag{9}$$

Ignoring terms of second order in the fluctuating parameters (e.g., $\delta\omega\zeta$), Eq. (9) becomes a complex Langevin equation:

$$\dot{\zeta}+[\Gamma - i\Delta]\zeta = (\gamma + i\delta\omega)\zeta_0, \tag{10}$$

where the atomic dephasing rate Γ is now seen to act as a viscous drag on the atom's ability to follow the rapidly fluctuating stochastic ''force'' $\delta\omega\zeta_0$. Integrating Eq. (10), we obtain

$$\zeta(t)=\zeta_0 e^{-(\Gamma - i\Delta)t} \int_0^t (\gamma + i\delta\omega) e^{(\Gamma - i\Delta)t'} dt'. \tag{11}$$

In the case of a nearly Lorentzian line shape, where we can assume that β is much greater than the atom's dephasing rate or laser detuning, the laser frequency fluctuations will appear to be δ correlated, so that $\langle \delta\omega(t')\delta\omega(t'')\rangle \cong 2\gamma\delta(t'-t'')$. Then, defining the autocovariance of atomic coherence fluctuations

$$C(t,t+\tau) \equiv \langle \zeta(t)\zeta^*(t+\tau)\rangle - \langle \zeta(t)\rangle\langle \zeta^*(t+\tau)\rangle, \tag{12}$$

it is straightforward to show from Eq. (11) that

$$\lim_{t\to\infty} C(t,t+\tau) \equiv C(\tau) = \left[\frac{\Omega^2\gamma}{16\Gamma[(\Gamma+\gamma)^2+\Delta^2]}\right] e^{-\Gamma|\tau|} e^{-i\Delta\tau}. \tag{13}$$

Each velocity subgroup in the vapor, however, will have its own autocovariance function owing to the different Doppler shifts of the atoms. Averaging Eq. (13) over the Doppler distribution of shifts in the case of the laser tuned to the center of the Doppler broadened line shape, and assuming that the Doppler width is much greater than the homogeneous linewidth, yields

$$\langle C(\tau)\rangle_\nu \cong \left[\frac{\Omega^2\gamma\sqrt{\pi\ln(2)}}{8\Gamma(\Gamma+\gamma)\Delta\nu_D}\right] e^{-(2\Gamma+\gamma)|\tau|}. \tag{14}$$

Taking the Fourier transform of $\langle C(\tau)\rangle_\nu$, we obtain the spectral density of coherence fluctuations, S_ζ, which is proportional to the spectral density of intensity fluctuations. Thus, at some Fourier frequency f within a small bandwidth Δf, the measured intensity noise is proportional to $\sqrt{\Delta f S_\zeta(2\pi f)}$, where

$$S_\zeta(\omega) = \int_{-\infty}^{\infty} \langle C(\tau)\rangle_\nu e^{-i\omega\tau} d\tau. \tag{15}$$

Evaluating the Fourier transform yields

$$S_\zeta(\omega) = \left[\frac{\Omega^2\gamma\sqrt{\pi\ln(2)}}{4\Gamma(\Gamma+\gamma)\Delta\nu_D}\right]\left[\frac{(2\Gamma+\gamma)}{(2\Gamma+\gamma)^2+\omega^2}\right], \tag{16}$$

so that

$$(\delta I/\langle I\rangle) = 8\sqrt{2\pi}kN\mu_{13}L\sqrt{\Delta f S_{\zeta}(2\pi f)}. \qquad (17)$$

Note that Eq. (16) predicts that, for Fourier frequencies much less than the atom's dephasing rate, the spectral density of intensity noise will be white.

The solid line in Fig. 6(b) corresponds to the intensity noise predicted by Eq. (16) at low Fourier frequencies, appropriately scaled to fit the computational data. Note that in the regime of small linewidths (i.e., $\gamma \ll \Gamma$), Eq. (16) predicts that the noise is proportional to $\sqrt{\gamma}$, while in the regime of very broad bandwidth fields (i.e., $\gamma \gg \Gamma$) the noise is proportional to $1/\sqrt{\gamma}$. Equation (13) provides the basic rationale for this nonmonotonic relationship between the RIN and laser linewidth. Though the variance of frequency fluctuations for a singlemode laser (i.e., phase diffusion field) scales like γ, the variance of atomic coherence fluctuations, which drive the RIN, has a nonlinear dependence on γ. In particular, for the homogeneous case of Eq. (13) the variance of atomic coherence fluctuations is maximized when $\gamma = \Gamma$.

VI. DISCUSSION

We have examined the influence of single-mode laser linewidth on PM-to-AM conversion experimentally, computationally and analytically. The significant result from these studies is that the efficiency of PM-to-AM conversion is a nonmonotonic function of laser linewidth. Basically, PM-to-AM conversion is driven by atomic coherence fluctuations, and the variance of these fluctuations (in the homogeneous case) has an extremum when the laser linewidth equals the atomic transition's homogeneous linewidth.

The results have an immediate bearing on recent attempts to improve the performance of gas-cell atomic clocks by using diode lasers for optical pumping. In the traditional gas-cell clock, a population imbalance between the ground-state hyperfine sublevels of Rb^{87} is achieved by optical pumping with a rf discharge lamp [23]. In the absence of a microwave field, resonant with the ground-state hyperfine splitting, the transmitted intensity of the discharge lamp is at a maximum. However, in the presence of resonant microwaves the hyperfine population imbalance is destroyed, and the transmitted intensity is minimized. Hence the intensity of transmitted light in this device provides the operative signal that is used to stabilize a microwave field to an atomic resonance.

The atomic clock's short-term performance is often couched in terms of the signal-to-noise ratio, and roughly a decade ago it was predicted that more efficient optical pumping with a diode laser would yield orders-of-magnitude improvement in clock stability [24]. Though experiments have repeatedly verified the superiority of diode lasers over rf-discharge lamps with regard to the magnitude of an atomic clock's signal, they have also indicated that PM-to-AM conversion noise can be orders of magnitude larger with standard diode lasers than with rf-discharge lamps [5]. Prior to the present work, this result was completely counterintuitive, as the linewidth of a standard diode laser is roughly 50 MHz [11], while that of a rf-discharge lamp is $\sim$2 GHz [25]. However, in light of the present results, and the fact that optical dephasing rates in gas cell atomic clocks are $\sim$100 MHz [26], it can be appreciated that the standard diode laser devices operate in a regime where $\gamma \sim \Gamma$, the worst possible situation for PM-to-AM conversion noise. Alternatively, PM-to-AM noise is considerably reduced by employing a rf-discharge lamp whose linewidth is much greater than the optical dephasing rate [27]. Clearly, for improved gas-cell atomic clock performance one should use a diode laser with a narrowed linewidth, gaining an advantage in atomic clock signal amplitude, while paying a minimal price in PM-to-AM conversion noise. We note that this is just the approach taken by Mileti *et al.*, who demonstrated a short-term performance for the gas-cell atomic clock that rivals that of the passive hydrogen maser [6].

ACKNOWLEDGMENT

This work was supported under U.S. Air Force Contract No. Fo4701-93-C-0094.

[1] W. V. Davis, M. Kauranen, E. M. Nagasako, R. J. Gehr, A. L. Gaeta, R. W. Boyd, and G. S. Agarwal, Phys. Rev. A **51**, 4152 (1995).
[2] M. Kauranen, A. L. Gaeta, R. W. Boyd, and G. S. Agarwal, Phys. Rev. A **50**, R929 (1994).
[3] R. Walser and P. Zoller, Phys. Rev. A **49**, 5067 (1994).
[4] T. Yabuzaki, T. Mitsui, and U. Tanaka, Phys. Rev. Lett. **67**, 2453 (1991).
[5] J. C. Camparo and W. F. Buell, in *Proceedings of the 1997 IEEE International Frequency Control Symposium* (IEEE, Piscataway, NJ, 1997), pp. 253–258.
[6] G. Mileti, J. Deng, F. L. Walls, D. A. Jennings, and R. E. Drullinger, IEEE J. Quantum Electron. **34**, 233 (1998).
[7] R. J. McLean, P. Hannaford, C. E. Fairchild, and P. L. Dyson, Opt. Lett. **18**, 1675 (1993).
[8] D. H. McIntyre, C. E. Fairchild, J. Cooper, and R. Walser, Opt. Lett. **18**, 1816 (1993).
[9] The acronym TJS stands for transverse junction stripe, and refers to the physical construction of the diode laser. See D. Botez, J. Opt. Commun. **1**, 42 (1980) for a more detailed discussion.
[10] EOSI is a company trade name. For a brief description of this commercial system, see M. Lang, Laser Focus World **32**, 187 (1996).
[11] J. C. Camparo, Contemp. Phys. **26**, 443 (1985); C. E. Wieman and L. Hollberg, Rev. Sci. Instrum. **62**, 1 (1991).
[12] W. Happer, Rev. Mod. Phys. **44**, 169 (1972).
[13] J. C. Camparo, J. Opt. Soc. Am. B **15**, 1177 (1998).
[14] O. S. Heavens, J. Opt. Soc. Am. **51**, 1058 (1961).
[15] See, for example, M. Nakamura, K. Aiki, N. Chinone, R. Ito, and J. Umeda, J. Appl. Phys. **49**, 4644 (1978).
[16] This value is consistent with expectations for this type of laser, if it is remembered that ASE represents a sum over all but the main lasing mode. See, for example, W. Susaki, T. Tanaka, H. Kan, and M. Ishii, IEEE J. Quantum Electron. **QE-13**, 587 (1977).

[17] A. P. Willis, A. I. Ferguson, and D. M. Kane, Opt. Commun. **122**, 31 (1995).

[18] See, for example, A. Yariv and W. M. Caton, IEEE J. Quantum Electron. **QE-10**, 509 (1974); S. N. Dixit, P. Zoller, and P. Lambropoulos, Phys. Rev. A **21**, 1289 (1980), and references therein.

[19] A. Papoulis (McGraw-Hill, New York, 1984).

[20] J. C. Camparo and P. Lambropoulos, Phys. Rev. A **47**, 480 (1993).

[21] W. Cheney and D. Kincaid, *Numerical Mathematics and Computing* (Brooks Cole, Monterey, CA, 1985); W. H. Press and S. A. Teukolsky, Comput. Phys. **6**, 188 (1992).

[22] R. H. Pennington, *Introductory Computer Methods and Numerical Analysis* (Macmillan, London, 1970).

[23] J. Vanier and C. Audoin, *The Quantum Physics of Atomic Frequency Standards* (IOP, Bristol, 1989), Vol. 2, Chap. 7.

[24] J. C. Camparo and R. P. Frueholz, J. Appl. Phys. **59**, 3313 (1986); IEEE Trans. Ultrason. Ferroelectr. Freq. Control **UFFC-34**, 607 (1987).

[25] T. Tako, Y. Koga, and I. Hirano, Jpn. J. Appl. Phys. **14**, 591 (1975).

[26] G. Missout and J. Vanier, IEEE Trans Instrum. Meas. **24**, 180 (1975).

[27] We note that a comparison of the laser's stochastic characteristics with the lamp's is complicated by the fact that the laser may be described as a phase diffusion field, while the lamp corresponds to a chaotic field. For a discussion of the different stochastic characteristics of these fields, see A. T. Georges and P. Lambropoulos, Phys. Rev. A **20**, 991 (1979).